

Flood Vulnerability Mapping and Risk Assessment Using Hydraulic Modeling and GIS in Tamanrasset Valley Watershed, Algeria

Housseyn Madi^{1,2*}, Ali Bedjaoui¹, Abdelghani Elhoussaoui³, Lala Oulad Elbakai², Aya Bounaama²

¹ LARHYSS Laboratory, University of Biskra, 7000, Algeria

² Faculty of Sciences and Technology, University of Tamanghasset, 11000 Algeria

³ Agence Nationale des Ressources Hydriques, Tamanghasset, 11000, Alegria

* Corresponding author's mail: housseyn_madi@yahoo.fr

ABSTRACT

The paper is focused on the integration of the US Army Corps of Engineers Hydrologic Engineering Center (HEC) models, particularly the HEC-RAS (River Analysis System) 1D hydraulic model, into a decision support system for predicting the effects of floods. The study was conducted in the Tamanrasset Valley watershed in Algeria, where the HEC-RAS model was used to calculate water flow profiles for various flood events that occurred downstream. The objective of the study was to generate flood maps for extreme river flood events in the area, which could help assessing the risk of flood vulnerability in the area study. The process involved using the HEC-RAS 1D model to simulate the water flow in the river, taking into account the various flow and boundary conditions. The results of the simulation were then exported and analyzed in GIS-based software, HEC-GeoRAS, to prepare the flood inundation maps. The flood maps were based on the water level at each cross-section, which was calculated using the water surface profiles generated by HEC-RAS. The study aimed to identify flood zones using a combination of HEC-GeoRAS and GIS. The HEC-GeoRAS extension was utilized in a GIS environment to determine flood zones associated with 10-year, 20-year, 50-year, and 100-year return periods. The results of the study confirmed the effectiveness of the integration of GIS and HEC-RAS and demonstrated the performance of the model. Based on these findings, the study recommends the application of this model in planning and management programs for both residential and agricultural areas, to ensure appropriate measures are taken for future flood defense.

Keywords: HEC-RAS; flood prediction; GIS; flood inundation maps; flood zones.

INTRODUCTION

Natural disasters are taking a toll on people and their properties, with floods and drought being the most frequent and impactful of them all. Floods, in particular, can happen in different areas, such as rivers, wadis, and also can occur in coastal regions, causing severe damage and loss of life when the water flow surpasses the maximum capacity of the river channel. Addressing the issue of inundation risk estimation and mitigation is therefore crucial in our current times (Zhang et al., 2014).

Floods are considered one of the most frequent types of natural disasters that can have

catastrophic impacts on both, local communities and infrastructure. (Porter et al., 2021). They can cause fatalities (Petrucci et al., 2019), significant economic damage (Merz et al., 2010), and disruptions to socioeconomic activities (Giannaros et al., 2020). For sustainable development, it is imperative to have reliable flood risk assessment and resilient urban planning. Despite advancements in flood mitigation techniques and technology, floods continue to pose a significant threat to human lives. (Sassi et al., 2019). This can be attributed to the increase in human settlements and also to the increase of economic assets situated in flood-prone areas, alterations in land usage, and the influence of the climate crisis (Sassi et al., 2019).

As noted by (Jonkman et al., 2008), it is essential to identify vulnerable areas and assess the factors and impacts of floods to forecast and control the destruction caused by such disasters. The risk of flooding can be determined by the occurrence probability of risings and their consequences (Raaijmakers et al., 2008). A comprehensive understanding of the situation enables not only risk management and measures to minimize life and material losses, but also allows for diverse possibilities for adapting the design of water supply engineering works, as described by (Breton and Marche, 2001).

In Algeria, The worst flood was the one that occurred on November 10th, 2001 in the Bab El Oued area of Algiers, with a maximum flood flow of 730 m³/s and a total flow of 2,600,000 m³ causing a damage of 772 deaths (Menad et al., 2012). Algerian flood studies are a mainly unknown field. There is a lack of data in the arid and Desert regions, and Algerian hydrological directories only include a small amount of data. Despite the importance of understanding flood events in these areas, the lack of information about flood series makes it difficult to draw comprehensive conclusions (Yamani et al., 2016).

Tamanrasset, among some towns in Algeria, faces many problems with traffic congestion, water use and flood rescue at the watershed scale is a major problem for local communities, agricultural lands and residents. The study area is very dry and is characterized by strong tectonic formations, climate change, Hydrological and hydraulic models have been used to simulate and predict floods and floods in watersheds by hydrologists to understand watershed behavior under the influence of several factors, such as increased urbanization (Emsalem, 1955).

The Wadi Tamanrasset in its downstream part towards the city has a relatively steep slope, generally around 0.7%. On 5th, August 1932, for a height of 30 cm and a width of 50 meters, the speed of the flow is estimated at 2 m/s, in a very turbulent way, with a significant solid flow (Emsalem, 1955). In this study, we map the flood-prone (at-risk) region in an arid area and then examine the tools for evaluating and mapping flood risk and its sources of uncertainty. Hydrological and hydrodynamic modeling with HEC-RAS is used to estimate the damage. The mapping of the flooded and at-risk areas in the examined area is presented last.

MATERIALS AND METHODS

Study area

The Tamanrasset Valley is located on the province of Tamanrasset (Figure 1), in the far southeast of Algeria, and it covers an area of 489.87 km² in its watersheds, and we are limited in this work to only one part that forms the most active section in the Tamanrasset Valley, which extends from ASSEKREM (2800 m) in the ATAKOR chain up The level of the city of Tamanrasset (1358 m) (Emsalem, 1955).

The State of Tamanrasset is located in the extreme south of the country Algeria; it borders with a country namely Niger and shares borders with IN SALAH, ADRAR; BORJ BAJI MOKHTAR; ILIZI; DJANET; and IN GUEZAM (Figure 2) Our study area is the Tamanrasset basin and is located between 5°30' and 5°41' East longitude, and between 22°46' and 23°15' North latitude. The average altitude is 1800 m.

The Tamanrasset Valley is located on the province of Tamanrasset (Figure 1), in the far southeast of Algeria, and it covers an area of 489.87 km² in its watersheds, and we are limited in this work to only one part that forms the most active section in the Tamanrasset Valley, which extends from ASSEKREM (2800 m) in the ATAKOR chain up The level of the city of Tamanrasset (1358 m) (Emsalem, 1955).

Overview of the flooding of the Wadi of Tamanrasset

The population growth in Tamanrasset resulted in intense urbanization and faced challenges due to the terrain; uncontrolled expansion of housing into the river bed has negatively impacted the flow of floods and increased the risk of destructive consequences. Table 2 lists the Tamanrasset Valley's most serious floods and the resulting major damages, including as deaths, injuries, and homeless.

2016 was characterized by significant rainfall, and the noteworthy day of 2016/08/10 saw a significant rainfall of approximately 79.7 millimeters in Asekrem Table 1. On this day, Tamanrasset city witnessed a valley flood (Figure 3), where the strong and heavy water of the valley broke the protective wall and the valley overflowed its path without causing harm.

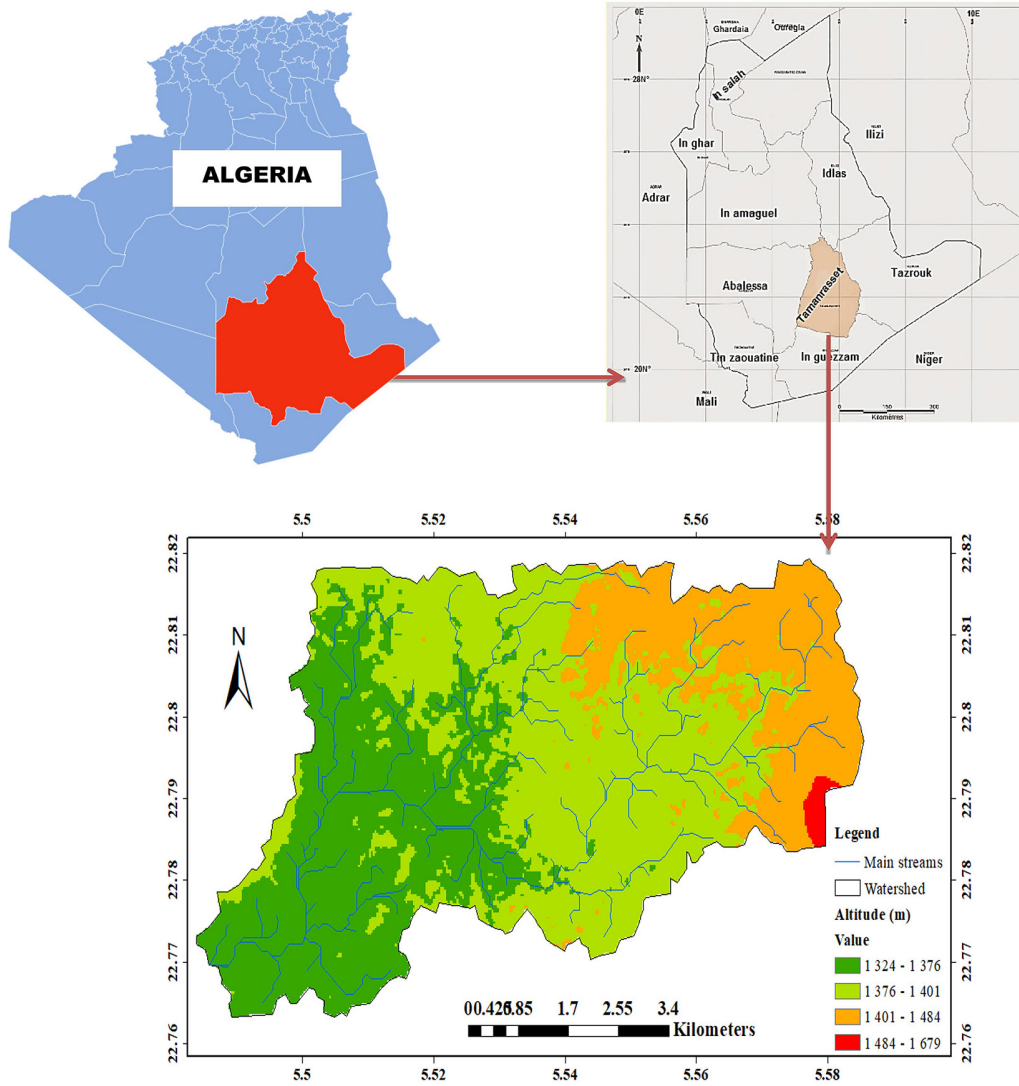


Figure 1. Geographical location of the study area

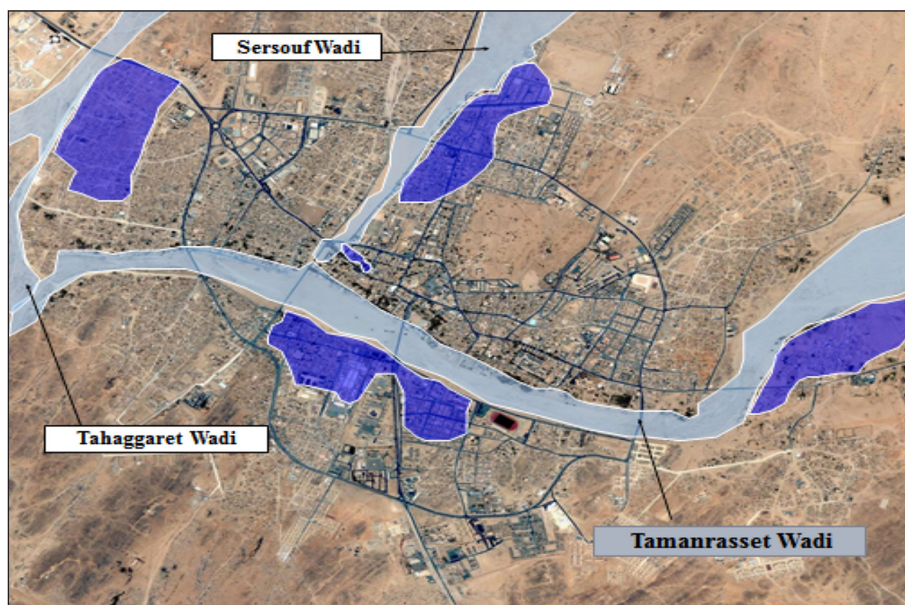


Figure 2. principals Wadis and the flooded zones in Tamanrasset Valley, according to civil defense unit of Tamanrasset (DGPC, 2016)(DGPC: Direction générale de la protection civil)

Table 1. Monthly average of precipitation during 2016

Month	Jan	Feb	Mar	Apr	May	Jun	Jul	Aug	Sep	Oct	Nov	Dec
Tamanrasset	0	0	0	0	1.6	13.3	47.2	36	0.5	0.4	0	0.1
Assekrem	0.3	0	0	0	40.1	12.6	27.7	79.7	1.6	4.8	9.1	0

Table 2. Most important floods during the last decade in the Tamanrasset Valley

Date	P(mm)	Type of flooding	Description of the disaster
Aout 1977	/	Strong enough	150 family affected 25 houses collapsed
Juil. 1997	60	Important	600 family affected All Tamanrasset's wadis have been flooded
Juil. 2000	35	Strong enough	09 Family affected
Aout 2015	40.3	Very strong	Water infiltration in several homes 23 roofs destroyed 52 houses completely destroyed 26 partially destroyed houses Distracted
Aug. 2018	95.6	Very important	Catastrophic damage to people's property, in particular constructions made of local materials. - Water infiltration in several homes - 963 families affected - 519 partially collapsed houses - 223 houses completely collapsed



Figure 3. Examples of damage caused by the flood of August 2016 (Photos taken by Civil Defense of Tamanrasset, Algeria, 2016) (DGPC, 2016)

The weather stations in Tamanrasset, and Asekrem recorded the rainfall according to the monthly average during the year as follows:

The topographical nature of some areas in the state makes them vulnerable to flood risk due to their lowlands or lack of vegetation cover (Madi et al., 2013), in addition to other factors such as the inability of water drainage systems to handle large amounts of water from heavy rains, non-compliance with building codes, sudden streams. All of this can result in floods that are proportional to the magnitude of the water flow. Moreover, the City of Tamanrasset is one of the regions affected by seasonal rains in the summer season (DGPC, 2016)*. Tamanrasset city is exposed to floods due to runoff from the slopes of the mountainous areas of the Assekrem, Hoggar and Adriane, that collect in the large Tamanrasset Wadi and Sersouf Wadi. This poses a danger to the Gataa Elouad, Sersouf, Tahaggaret and Tafsit Valley (Figure 2). Figure 3 shows examples of flood damage in Tamanrasset City in August 2016.

According to a report made by Direction of civil Defense of Tamanrasset state in 2017, the city of Tamanrasset is exposed to floods due to the runoff of the wadis from the slopes of the Askarem, and Adriane mountains, which converge in the Tamanrasset and Sersouf valleys. This poses a danger to the residents. Due to its proximity to the wadis and the porous nature of the building materials (brick), the Tamanrasset valley often experiences the washing away of vehicles trying to cross the valley, which

can result in material and human losses. Additionally, the water pools are filled and used for swimming by citizens, leading to cases of drowning. This phenomenon applies to all the population centers in the municipalities of the Tamanrasset state, according to related statistics (DGPC, 2016).

Hydrographic network

In the Tamanrasset region, water availability is sourced from natural, permanent, semi-permanent water points, and underground waters. However, despite these sources, the scarcity of water in this region is a significant issue, as it is associated with high temperatures and constant hot and dry winds. These conditions result in difficult living conditions for wildlife and human populations, as well as their livestock (Hamdine, 2001). The wadis, or seasonal watercourses, in the Tamanrasset region primarily originate in the central Hoggar area, which is the main area of water distribution. Among these wadis, two are particularly significant: the Igharghar wadi and the Tamanrasset wadi. These large quaternary wadis are responsible for draining the waters from the west and the north of the region (Raeli et al., 2016).

The Tamanrasset Wadi watershed has an elongated shape with an average elevation ranging from 1300 to 2700 m and an average slope of 0.84%. The relief is classified as moderate, with a weak to average aspect and an overall slope of 0.21% (Ig).

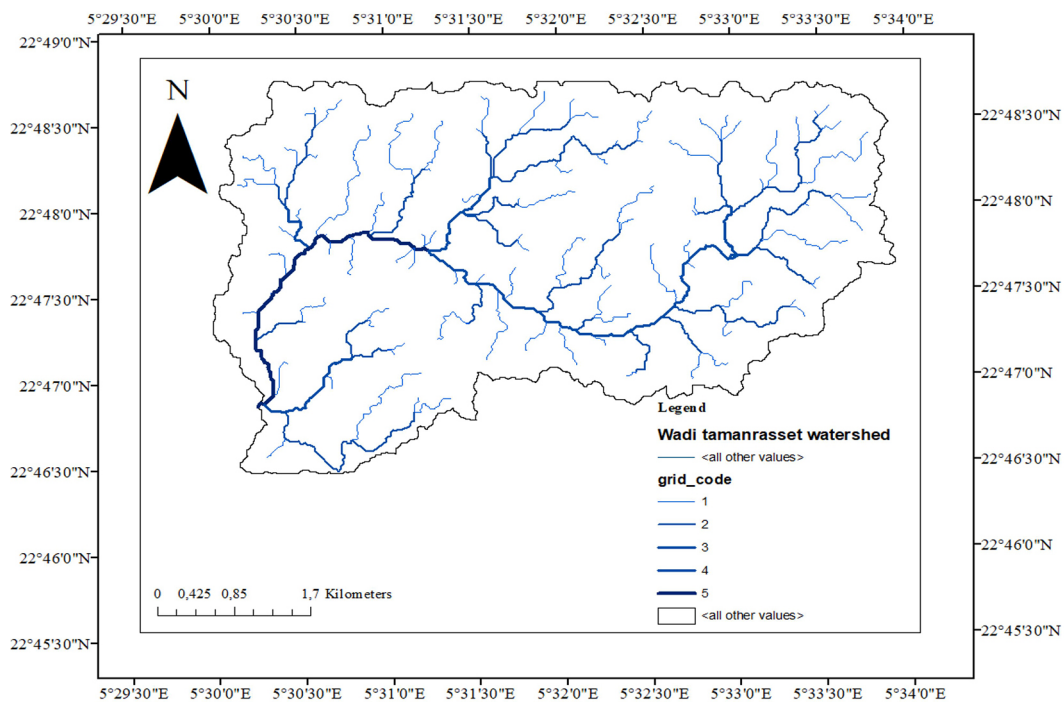


Figure 4. Hydrographic network of Tamanrasset Wadis

Table 3. Characteristic of the basin of Oued Tamanrasset

Characteristic	Parameter	Unit	Symbol	Value
Morphology of the watershed	Area	Km ²	A	458.9
	Perimeter	Km	P	132.16
	Compactness index	-	Kc	1.72
	Length	Km	L	58.77
	Width	Km	I	7.81
Relief	Max altitude	m	Hmax	2900
	Average altitude	m	Hmoy	1201
	Min altitude	m	Hmin	1300
	Global slope index	-	Ig	0.21
	Average slope index	-	Ip	0.84
Hydrographic network	Length of the main Talweg	Km	Lp	68.23
	Total length of tributaries	Km	L	233.21
	Concentration time	h	Tc	10.50
	Runoff velocity	Km/h	V	6.49
	Drainage density	Km/Km ²	Dd	0.14

The drainage density of the basin is 0.14 km/km², indicating poor drainage due to its geological and lithological features (see Table 3). The study area is characterized by highly tectonized formations with upstream basaltic and downstream granite nature. The Figure 4 represents the hydrographic network of Tamanrasset Wadis.

Climate and precipitation

The number of weather stations in the state of Tamanrasset is limited, with only two stations

present (Table 4). Despite this, the coverage of climatic stations in the study region is limited.

In this work, a pluviometric series of maximum daily precipitation measurements is used to provide an insight into the hydrological behavior of the Tamanrasset watershed over a long period of time. The precipitation data, which covers the period from 1953 to 2019, was obtained from the National Office of Meteorology and spans 66 years (Table 4). The analysis of this meteorological data will help to determine the relationship between precipitation and potential floods in the

Table 4. Characteristics of weather stations of the city of Tamanrasset

Station kind	Coordonnées			
	Latitude	Longitude	Altitude (m)	Period
Tamanrasset	22°47'N	5°31'E	1362	1953/54–2019/20
Assekrem	23°16'N	5°38'E	2710	1953/54–2019/20

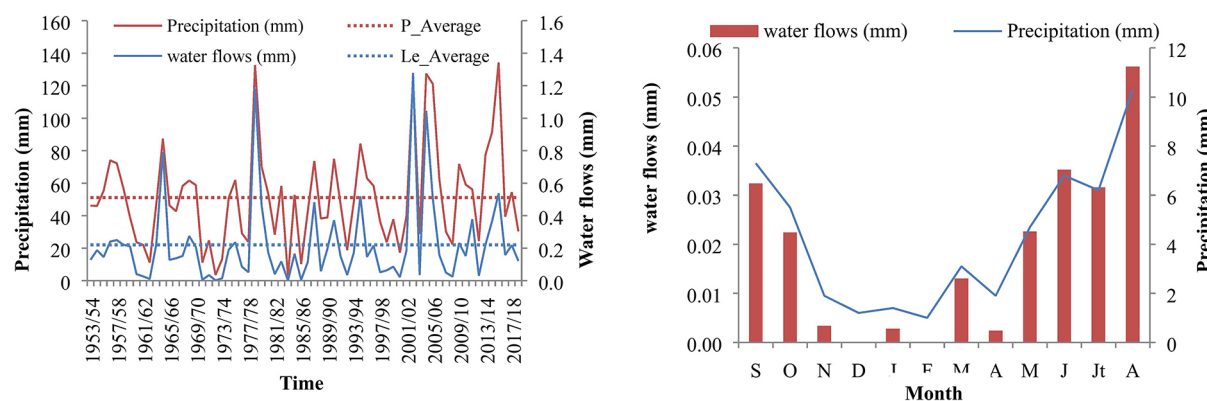


Figure 5. Interannual rainfall and water flows variability

area. The use of long-term precipitation data is crucial in understanding the hydrological behavior of the Tamanrasset watershed.

The collected precipitation and flow rate data from the 66-year period exhibits significant yearly variations. 2015–2016 was a remarkable year, with a record high of 134.3 mm of precipitation and 1mm of flow rate, whereas 1983–1984 saw the lowest recorded values of 2.5 mm of precipitation and zero flow rate (Figure 5). The average precipitation stands at 51.4 mm, while the average flow rate is 0.22 mm. Winter is the driest season while summer experiences the highest levels of precipitation, with the majority of the flow taking place in August. These fluctuations highlight the need for monitoring and modeling the Tamanrasset watershed to better understand the impact on water resources and flood risk (Emsalem, 1955).

Methodology of investigation

The findings of the rising phenomena in the region may be analyzed using a variety of approaches to map the flood risks. In general, three basic techniques can be used: historical and paleo-hydrologic techniques (De Wrachien et al., 2011), hydro-geomorphologic techniques, and hydrological-hydraulic techniques (Lastra et al., 2008). We decided to use the latter approach, and as a result, the following four steps were taken.

The first step in the process is to conduct a statistical analysis of the precipitation data collected in the period of study. The second step is quantifying the projected flow through Hydrological

modeling, which is based on Empirical models. In the third step, the HEC-RAS software is used for hydraulic modeling, which enables us to calculate the rising hydrographs. This step involves hydraulic modeling based on the HEC-RAS, which uses data such as land use maps and a DEM (digital elevation model), as well as flow calculations from the hydrological model. Finally, we involves mapping the vulnerable zones by intersecting the flood level determined by HEC-RAS software and the DEM model with the original ground level to form a horizontal plane that represents the flooded area.

Hydrological modeling

The hydrological modeling principle is also known as model rain-flow. This method transforms a series of weather conditions in a catchment area, such as precipitation and soil moisture, into a series of flows. Rain is converted into a hydrogram of rising by applying two functions in succession. The first one is the production function used to determine the clear rain hydrogram from the rough rain. The second one is, the transfer function, that aims to assess the rising hydrogram resulting from the clear rain (Benaoudj, 2014).

The IDF (intensity-duration-frequency) curves are created to summarize the precipitation information at the representative station of the study area. These curves enable the calculation of short-term flows and estimation of rainfall and runoff flows, defining the uniform rainfall with a constant intensity throughout its duration (Yamani et al., 2016). The IDF curves are plotted for

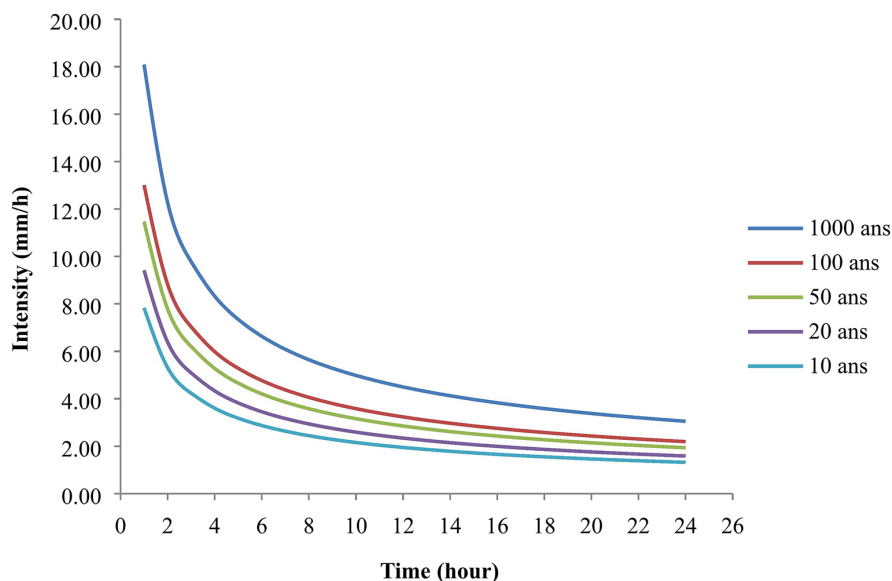


Figure 6. Curves IDF “Intensity-Duration-Frequency”

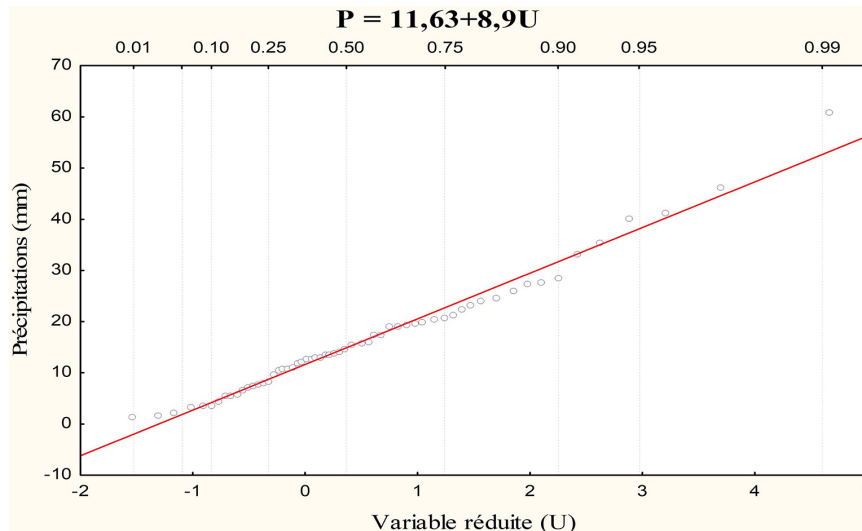


Figure 7. Gumbel distribution fitting graph

different return periods of, 10, 50, 100 and 1000 years (Figure 6).

In this study, hydrological data is essential for the model’s calibration and validation. Flood hazard mapping was conducted using flood magnitude (m^3/s) based on the Gumbel distribution (Figure 7) for return periods of 10, 20, 50, 100 and 1000 years. However, the contribution of flood from the tributaries of the Wadi Tamanrasset was not included in the model due to the absence of gauge stations.

The calculation of flood levels is influenced by the availability of data. The selected method is related on the unique conditions and data, and is often determined by the researcher. This study utilized empirical formulas such as Mallet-Gauthier,

Giandotti, Turazza, Sokolovsky, and the rational method to estimate peak flood flows based on morphological and pluviometric data. These formulas were deemed suitable for small catchment areas.

Giandotti formulas

Giandotti method utilizes the laws of runoff and incorporates both the morphometric characteristics of the catchment area and the time of concentration to determine flood peaks. This formula has been found to give particularly accurate results for mountainous basins.

$$Q_{max} = \frac{C.S.h_{tc,p\%} \cdot \sqrt{h_{moy} - h_{min}}}{4\sqrt{S} + 1.5L} \quad (1)$$

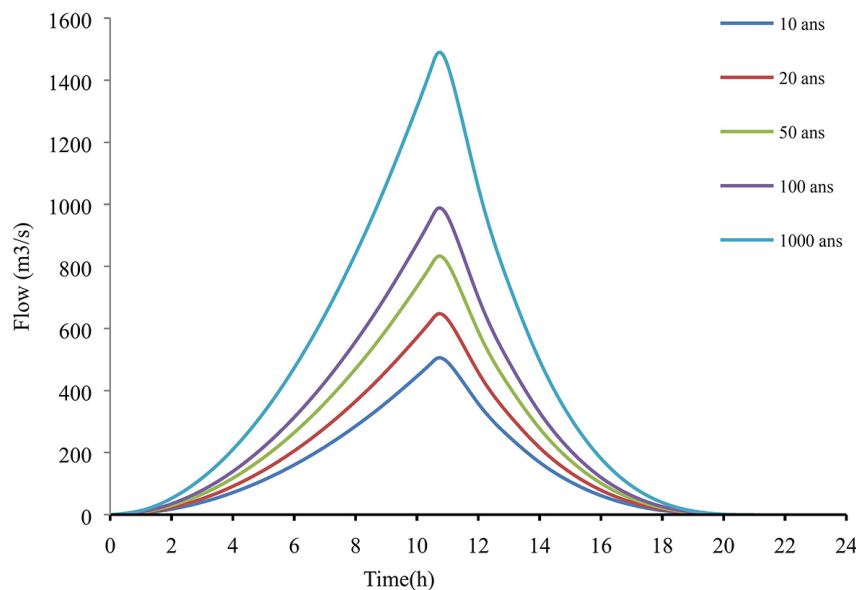


Figure 8. Flood hydrogram for different return periods

Table 5. Point flow “Qp” for different return periods (GIANDOTTI’s formula)

Return period (year)	Rain of t_c duration (P_{tc})			Peak flow Q_p (m ³ /s)		
	Tamanrasset	Assekrem	Average	Tamanrasset	Assekrem	Average
1000	73.24	241.89	157.57	504.5	1666.3	1085.42
100	52.66	173.05	112.86	362.8	1192.1	777.43
50	46.44	152.21	99.33	319.9	1048.5	684.22
20	38.12	124.21	81.17	262.6	855.6	559.12
10	31.7	102.93	67.32	218.4	709.1	463.71

where: s – area of the catchment (Km²);

L – length of the main Talweg (km);

h_{moy} – average altitude in m;

h_{min} – minimum altitude (m);

$h_{tc,p\%}$ – depth of water precipitated for a given probability and the time of concentration of the flow;

C – topographic coefficient varying between 0.066 and 0.166.

Giandotti Finding the return period discharges is the goal of the formula mentioned in the equation above. The estimated discharges that occurred during each return period is shown in Table 5 and Figure 8.

Hydraulic and flood plain modeling

In the hydrodynamic modeling of a river with floodplains, numerical simulations are necessary to solve the conservation equations for free surface flow. The fact that these models adequately depict the morphology of the river channel and its adjacent floodplains is a crucial feature. (Casas et al., 2006). A number of numerical techniques, including one-, two-, and three-dimensional methods (Yamani et al., 2016, Bladé et al., 2014) can be used for modeling rivers and floodplains. These models vary in terms of their capacities and data collection process. In this work, HEC-RAS model was chosen depending on the meteorological and geospatial data available in the study region.

The U.S. Army Corps of Engineers developed the windows-based hydraulic tool known as the HEC-RAS Model. For a complete network of naturally occurring and artificially created channels, it performs one-dimensional hydraulic calculation and determines the water surface heights at all important areas using up with data. (Rivera et al., 2007). This is accomplished by determining the subcritical flow at each cross-section using the Bernoulli Equation 1. (Huber, 2012)

$$Z_1 + Y_1 + \frac{\alpha_1 V_1^2}{2g} =$$

$$= Z_2 + Y_2 + \frac{\alpha_2 V_2^2}{2g} + \Delta h \quad (2)$$

where: the elevation of the channel inverts at two different cross-sections is represented by Z_1 and Z_2 . The water depth at these cross-sections is represented by Y_1 and Y_2 , respectively. The mean flow velocity at the two cross-sections is represented by V_1 and V_2 . The velocity coefficients at the two cross-sections are represented by α_1 and α_2 . The gravitational acceleration is represented by g . The energy head loss between the two cross-sections is represented by Δh .

HEC-GeoRAS, which is coupled with ArcMap, is used to create floodplain maps. Water levels at each cross-section are obtained using HEC-RAS to generate the inundation maps.

With a triangulated irregular network (TIN) constructed from a digital elevation model (DEM), spatial geometric data properties are recovered. The reach between two adjacent cross-sections is measured using flow route centerlines, which also serve to indicate the center of mass of the river’s flowing water (Jagadeesh and Veni, 2021). After entering the geometric data into HEC-RAS, the simulation results are processed and exported using HEC-GeoRAS for post-processing and GIS-based analysis. Flow and boundary conditions are then entered. As the region had significant precipitation, interannual changes in water flows (Figure 5) comparatively demonstrate a considerable run out of water flow.

After tracing wadi of Tamanrasset in ArcGIS software, we used HEC-RAS software (Figure 9) to carry out the numerical simulation of their floods. We selected the hydrograph flood discharges calculated by the GIANDOTTI formula corresponding to return time of 10 years,

50 years, 100 years, and 1000 years (Figure 8). HEC-RAS software is a hydraulic simulation tool for rivers and canals. It allows the evaluation of water discharges and heights at all sections of a river (Modeling a river with HEC-RAS). Several studies of arid and Desert regions have using HEC RAS, such as in (Hafnaoui et al., 2020; Abdessamed and Abderrazak; 2019; Jagadeesh and

Veni, 2021; Yamani et al., 2016). The geometric data involves defining the connectivity of the river system and is used to present the flow data that moves from the source to the downstream section under study (Figures 9, 10), considering boundary conditions to determine the water level at the limits of the river such as the upstream and the downstream.

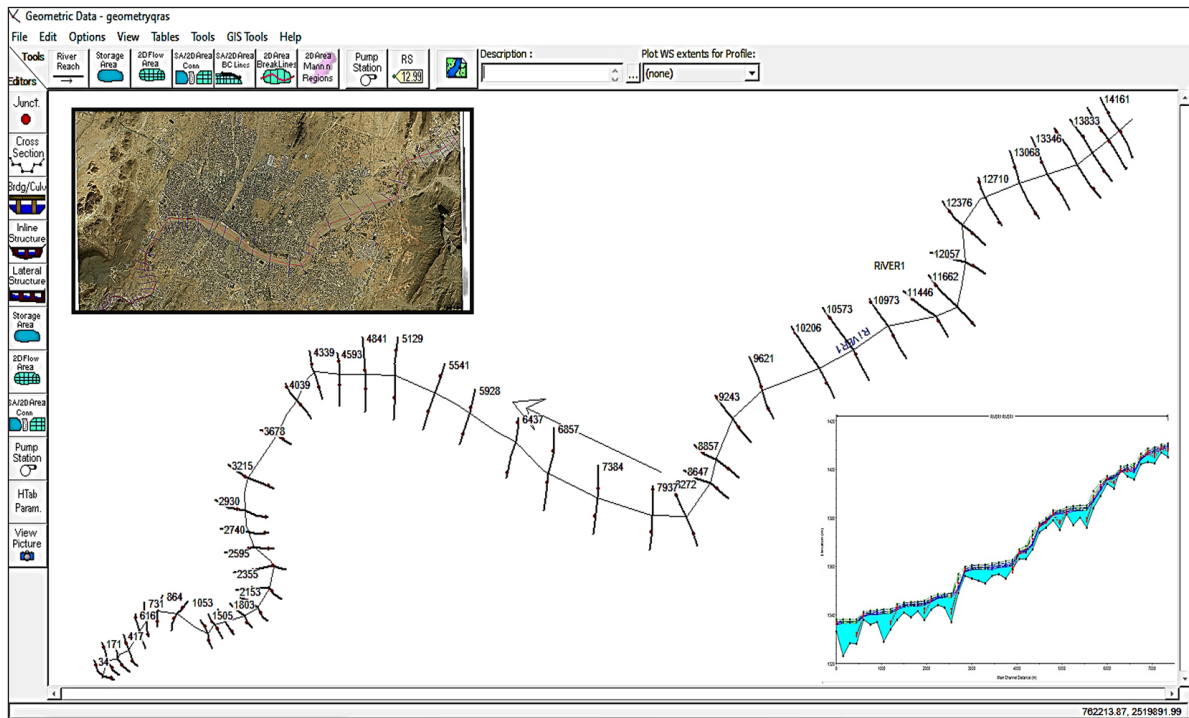


Figure 9. Geometrical data model setup by HEC-GeoRAS

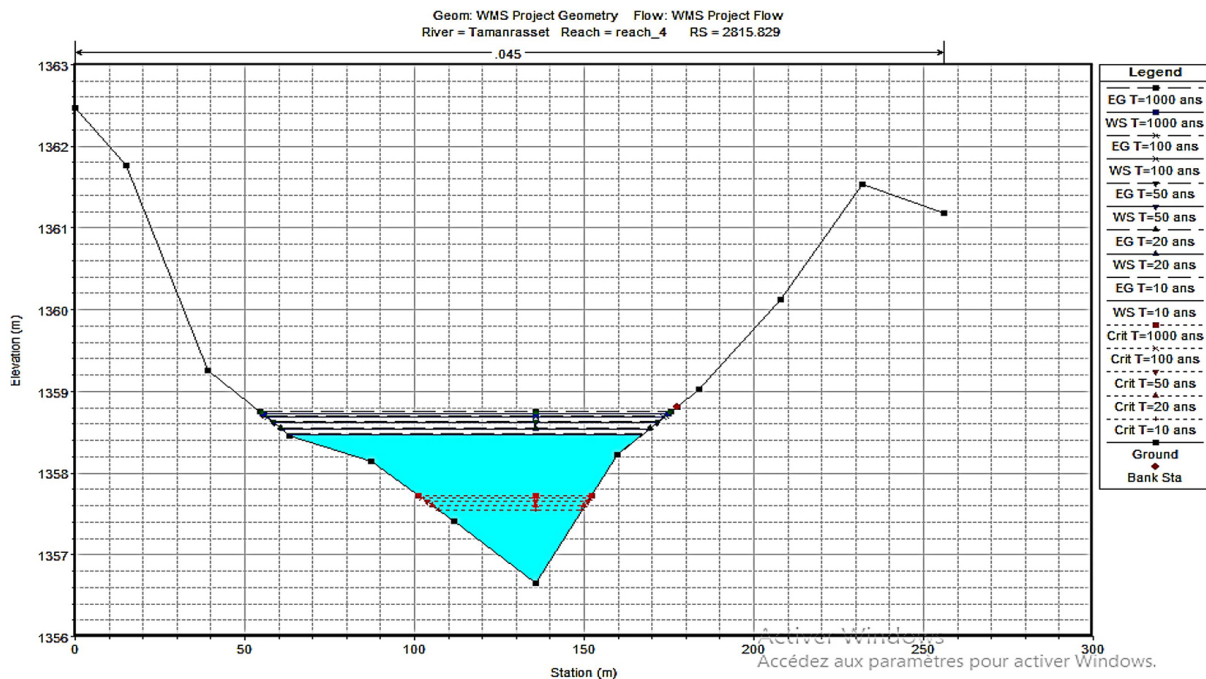


Figure 10. Example of Cross section of the Wadi of Tamanrasset

RESULTS AND DISCUSSIONS

The topographic to raster interpolation method in HEC-GeoRAS is used to overlay the flood water levels acquired from HEC-RAS output onto the study area’s land surface elevation. The depth of inundation is calculated using the difference between land elevation surfaces and water level interpolation. (Figure 4). The average decrease in precipitation, i.e. 0.06% compared to the Interannual average, The deficits recorded mainly relate to the wet season, to 5.63% for the rains, the downward trend is of course much more noticeable on the ‘Assekrem than on Tamanrasset. A dry season lasts from November to April (or May) while a wet (flood) season lasts from June

to September (or October). The summer or rainy season, often known as flood season, is when more than 80% of the rainfall takes place. Maps of flood inundation are only created during flood seasons for this study.

Areas affected during floods were identified by mapping these areas after extrapolation from a GIS program (HEC-RAS). To highlight this danger in the middle of the Tamanrasset valley, we recreated the layers of the water extension that intersected with the regions on the basis of a topographic map, and corrected it using a satellite navigator that allows visualization of the affected areas. The maps presented on the Figures 11–13 shows the results of the numerical simulation of the floods in the Tamanrasset wadi for each return period. The floods occurring every 10, 50, one 1000, or one 1000 years inundate the surface area indicated in the Table 6. There is a successive increase in the flooded zone for each return period.

Small areas reported higher flooding in June and August as a result of a steady rise in rainfall intensity. These maps show that this district saw the most flooding in the month of August. These

Table 6. Inundated area in hectare (Ha)

Return period (years)	Area (ha)
10	96
50	107.3
100	111.9
1000	122.9

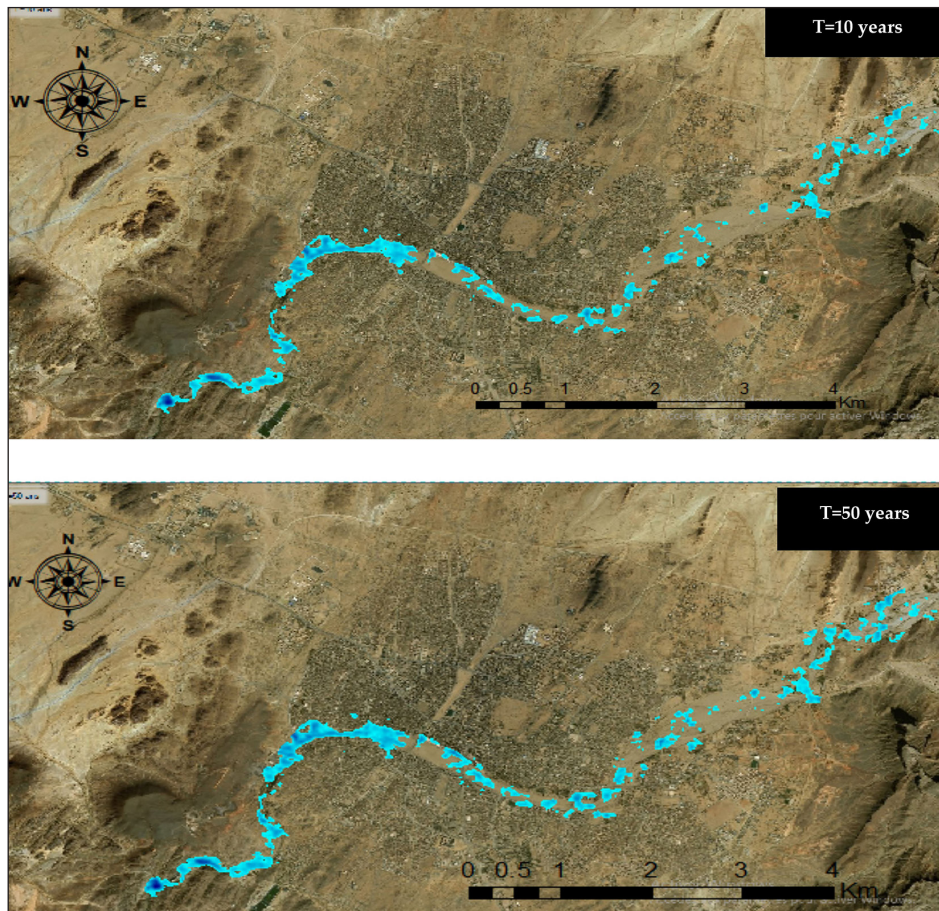


Figure 11. Flood Inundation map developed by model simulation at City of Tamanrasset Valley watershed for 10 and 50 return period

areas were fully submerged by floodwaters on August 5, 2020, the outlet considered to be the most dangerous place in the event of flooding, because this area receives part of the main water

course. Consequently, Part of low risk in the center of the wadi.

The dwelling of the city of Tamanrasset which impaled in the north-west side of the city receives

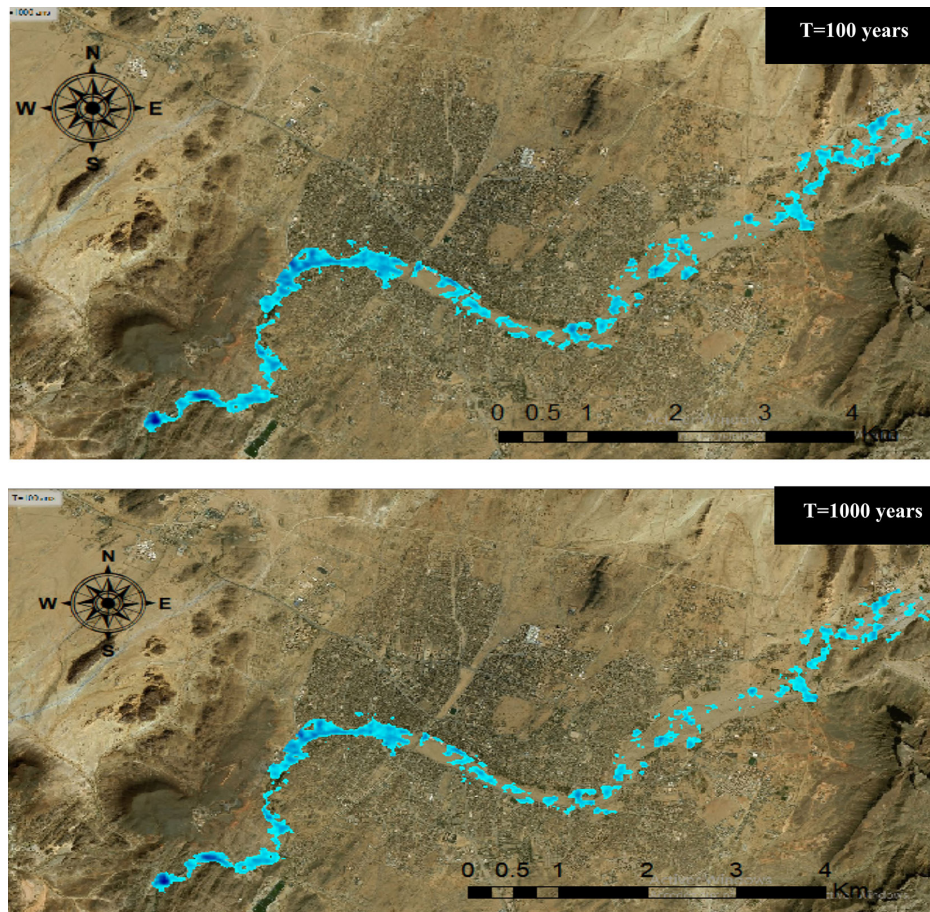


Figure 12. Flood inundation map developed by model simulation at City of Tamanrasset Valley watershed for 100 and 1000 return period

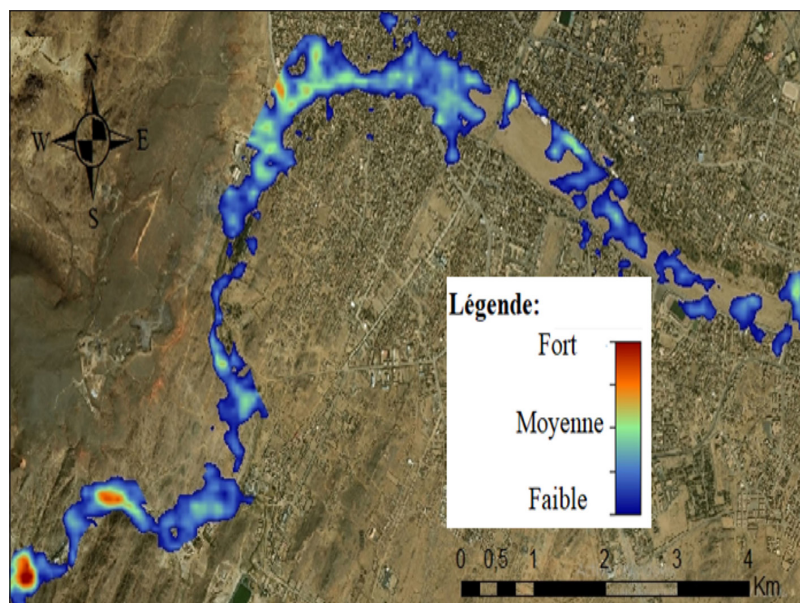


Figure 13. Flood vulnerability map

the average risk of flooding because their position under the slope. Floodwater naturally travels toward downward slopes, flooding the region with lower elevations. The case of the bridge with culverts in the center of Tamanrasset, which is almost 160 meters long. Floodwaters often flood the road over the bridge with every major flood pass.

This study discovered that the main channel experienced the highest speeds, up to 10 m/s, and that these velocities decreased as the water expanded onto the overlying banks. Less than 3.5 m/s and 0 m/s are the closing velocities in the over banks (both left and right) close to the model boundary. This outcome is acceptable due to the fact that the velocity is always greater in the center and decreases toward the border when examining the velocity distribution in a trapezoidal open channel (Akan, 2006).

CONCLUSION

The objective of this study was to analyze the factors contributing to the environmental phenomenon of floods in Tamanrasset, evaluate its susceptibility to flooding, and identify areas at risk of flooding. The study involved hydrological calculations of flood flows using data from the Tamanrasset station. Based on the vulnerability map to floods, we created a map that classifies the area into three zones according to the level of risk (high, medium, and low) to determine the limits of the flooded areas. In the subject of this work, stochastic modeling of Tamanrasset Wadi flood occurred in different return period was assessed with the aim of delineation probabilistic flooded areas. HEC-RAS applied as a one-dimensional Modeling System, which responded to the present project needs considerably.

The flood maps created in the present study can be used as a valuable reference for management of flood risk in the Tamanrasset region, with relevant technical services taking responsibility for its implementation. However, the lack of hydrometric data remains a significant obstacle for researchers in verifying their findings, particularly in terms of forecasting and modeling for Ungauged basins and predicting submerged areas. To address this, the researchers recommend the integration of both hydrological and hydraulic models. At the end of this study, it was found that the city of Tamanrasset is not adequately protected against floods. Therefore, it is necessary to

establish a protection system as soon as possible to reduce the effect of this hazard on human live, economic, and material assets, particularly in the areas affected first.

Acknowledgments

The authors gratefully acknowledge the support provided by the LARHYSS laboratory (University of Biskra, Algeria) in the form of materials, which were essential to the successful completion of this research project.

REFERENCES

1. Abdessamed, D., Abderrazak, B. 2019. Coupling HEC-RAS and HEC-HMS in rainfall–runoff modeling and evaluating floodplain inundation maps in arid environments: case study of Ain Sefra city, Ksour Mountain. SW of Algeria. *Environ. Earth Sci.* 78, 586. <https://doi.org/10.1007/s12665-019-8604-6>
2. Akan, A.O. 2006. *Open channel hydraulics*. Butterworth-Heinemann, Amsterdam Boston Heidelberg.
3. Bates, P.D., De Roo, A.P.J. 2000. A simple raster-based model for flood inundation simulation. *J. Hydrol.* 236, 54–77. [https://doi.org/10.1016/S0022-1694\(00\)00278-X](https://doi.org/10.1016/S0022-1694(00)00278-X)
4. Benaoudj, A. 2014. *Les Inondations Dans La Vallee Du M'zab: Genese Et Prediction* 15.
5. Bladé, E., Cea, L., Corestein, G. 2014. Modelización numérica de inundaciones fluviales. *Ing. Agua*, 18, 71–82. <https://doi.org/10.4995/ia.2014.3144>
6. Breton, C., Marche, C. 2001. Une aide à la décision pour le choix des interventions en zone inondable. *Rev. Sci. Eau J. Water Sci.* 14, 363–379. <https://doi.org/10.7202/705424ar>
7. Casas, A., Benito, G., Thorndycraft, V.R., Rico, M. 2006. The topographic data source of digital terrain models as a key element in the accuracy of hydraulic flood modelling. *Earth Surf. Process. Landf.* 31, 444–456. <https://doi.org/10.1002/esp.1278>
8. De Wrachien, D., Mambretti, S., Schultz, B. 2011. Flood management and risk assessment in flood-prone areas: Measures and solutions. *Irrig. Drain.* 60, 229–240. <https://doi.org/10.1002/ird.557>
9. Emsalem, R. 1955. Jean Dubief, Essai sur l'hydrologie superficielle au Sahara. *Géocarrefour* 30, 77–78.
10. Giannaros, C., Kotroni, V., Lagouvardos, K., Oikonomou, C., Haralambous, H., Papagiannaki, K. 2020. Hydrometeorological and Socio-Economic Impact Assessment of Stream Flooding in Southeast Mediterranean: The Case of Rafina Catchment (Attica,

- Greece). *Water*, 12, 2426. <https://doi.org/10.3390/w12092426>
11. Hafnaoui, M.A., Hachemi, A., Said, M.B., Noui, A., Fekraoui, F., Madi, M., Mghezzi, A. 2013. Vulnérabilité aux inondations dans les régions sahariennes - cas de doucen, 8.
 12. Hafnaoui, M.A., Madi, M., Hachemi, A., Farhi, Y. 2020. El Bayadh city against flash floods: case study. *Urban Water J.* 17, 390–395. <https://doi.org/10.1080/1573062X.2020.1714671>
 13. Hamdine, D.O. 2001. Conservation du Guépard (*Acinonyx jubatus* Schreber, 1776) dans les régions de: l'Ahaggar et du Tassili N'Adjer (En Algérie).
 14. Huber, W.C. 2012. Hydrologic Modeling Processes of the EPA Storm Water Management Model (SWMM), 1–10. [https://doi.org/10.1061/40685\(2003\)164](https://doi.org/10.1061/40685(2003)164)
 15. Jagadeesh, B., Veni, K.K. 2021. Flood Plain Modelling of Krishna Lower Basin Using Arcgis, Hec-Georas And Hec-Ras. *IOP Conf. Ser. Mater. Sci. Eng.* 1112, 012024. <https://doi.org/10.1088/1757-899X/1112/1/012024>
 16. Jonkman, S.N., Bočkarjova, M., Kok, M., Bernardini, P. 2008. Integrated hydrodynamic and economic modelling of flood damage in the Netherlands. *Ecol. Econ., Special Section: Integrated Hydro-Economic Modelling for Effective and Sustainable Water Management*, 66, 77–90. <https://doi.org/10.1016/j.ecolecon.2007.12.022>
 17. Lastra, J., Fernández, E., Díez-Herrero, A., Marquín, J. 2008. Flood hazard delineation combining geomorphological and hydrological methods: an example in the Northern Iberian Peninsula. *Nat. Hazards*, 45, 277–293. <https://doi.org/10.1007/s11069-007-9164-8>
 18. Madi, H., Mouzai, L., Bouhade, M. 2013. Plants cover effects on overland flow and on soil erosion under simulated rainfall intensity. *Int. J. Environ. Ecol. Eng.* 7, 561–565.
 19. Menad, W., Douvini, J., Beltrando, G., Arnaud-Fassetta, G. 2012. Evaluer l'influence de l'urbanisation face à un aléa météorologique remarquable : les inondations des 9-10 novembre 2001 à Bab-el-Oued (Alger, Algérie). *Géomorphologie Relief Process. Environ.* 18, 337–350. <https://doi.org/10.4000/geomorphologie.9954>
 20. Merz, B., Kreibich, H., Schwarze, R., Thielen, A. 2010. Review article "Assessment of economic flood damage." *Nat. Hazards Earth Syst. Sci.* 10, 1697–1724. <https://doi.org/10.5194/nhess-10-1697-2010>
 21. Naiji, Z., Mostafa, O., Amarjouf, N., Rezqi, H. 2021. Application of two-dimensional hydraulic modelling in flood risk mapping. A case of the urban area of Zaio, Morocco. *Geocarto Int.* 36, 180–196. <https://doi.org/10.1080/10106049.2019.1597389>
 22. Petrucci, O., Aceto, L., Bianchi, C., Bigot, V., Brázdil, R., Pereira, S., Kahraman, A., Kılıç, Ö., Kotroni, V., Llasat, M.C., Llasat-Botija, M., Papagiannaki, K., Pasqua, A.A., Řehoř, J., Rossello Geli, J., Salvati, P., Vinet, F., Zézere, J.L. 2019. Flood Fatalities in Europe, 1980–2018: Variability, Features, and Lessons to Learn. *Water*, 11, 1682. <https://doi.org/10.3390/w11081682>
 23. Porter, J.R., Shu, E., Amodeo, M., Hsieh, H., Chu, Z., Freeman, N. 2021. Community Flood Impacts and Infrastructure: Examining National Flood Impacts Using a High Precision Assessment Tool in the United States. *Water*, 13, 3125. <https://doi.org/10.3390/w13213125>
 24. Raaijmakers, R., Krywkow, J., van der Veen, A. 2008. Flood risk perceptions and spatial multi-criteria analysis: an exploratory research for hazard mitigation. *Nat. Hazards*, 46, 307–322. <https://doi.org/10.1007/s11069-007-9189-z>
 25. Raeli, M., Ceglie, V., Baourakis, G., Agrokippio, A. 2016. Monitoring vegetation and surface water dynamics of Wadi Tamanrasset using earth observation data - Sécheresse info.
 26. Rivera, S., Hernandez, A., Ramsey, R., Suarez, G., Rodriguez, S.A. 2007. Predicting flood hazard areas: A SWAT and HEC-RAS simulations conducted in aguan river basin of honduras, central America, 2, 594–603.
 27. Sassi, M., Nicotina, L., Pall, P., Stone, D., Hilberts, A., Wehner, M., Jewson, S. 2019. Impact of climate change on European winter and summer flood losses. *Adv. Water Resour.* 129, 165–177. <https://doi.org/10.1016/j.advwatres.2019.05.014>
 28. Yamani, K., Hazzab, A., Sekkoum, M., Slimane, T. 2016. Mapping of vulnerability of flooded area in arid region. Case study: area of Ghardaïa-Algeria. *Model. Earth Syst. Environ.* 2, 147. <https://doi.org/10.1007/s40808-016-0183-x>
 29. Zhang, Q., Gu, X., Singh, V.P., Xiao, M. 2014. Flood frequency analysis with consideration of hydrological alterations: Changing properties, causes and implications. *J. Hydrol.* 519, 803–813. <https://doi.org/10.1016/j.jhydrol.2014.08.011>